Order and Disorder in *p*-Dialkylbenzene–Urea Inclusion Compounds

S. C. Mayo, T. R. Welberry,[1] M. Bown, and A. Tarr

Research School of Chemistry, Australian National University, Canberra, ACT 0200, Australia

X-ray diffraction measurements of a series of dialkylbenzene–urea inclusion compounds have shown complex three-dimensional ordering of the guest molecules within the urea host. In four of the compounds large commensurate superstructures are observed, characterized by doubling of the *a* and *b* axes of the urea host substructure and a severalfold increase in the host *c* axis. Low-temperature phase transitions have been observed in all of these compounds corresponding to either monoclinic or orthorhombic distortions of the cell from the metrically hexagonal room temperature form. Possible structural arrangements for these compounds are discussed. © 1998 Academic Press

1. INTRODUCTION

1.1. Structural Features

It has long been known that urea will cocrystallize with suitable long-chain guest molecules to form host–guest inclusion structures (1, 2). In such compounds the urea host forms a framework of hexagonal tunnels parallel to the crystallographic *c* axis, occupied by guest molecules such as long-chain alkanes and their derivatives.

Nearly all urea inclusion compounds exhibit considerable disorder of the guest molecules, including both rotational disorder of the molecules about the tunnel axis and longitudinal disorder of the guests along the tunnels. The longitudinal disorder arises from the lack of a fixed relationship between the positions of the guest molecules in adjacent tunnels—the only periodicity of the guests being that within a given tunnel corresponding to the length of the guest molecule plus the intermolecular spacing. Hence, to a first approximation the guest molecules form an array of one-dimensional crystals with no correspondence of their origins, but with a regular spacing in the perpendicular direction due to the constraints of the host tunnels. This arrangement of the guest molecules results in an X-ray diffraction pattern characterized by sharp planes of diffuse intensity perpendicular to the *c** axis with a spacing corresponding to c_g, the periodicity of the guests along the tunnels

(Fig. 1) (3). In many cases, however, intensity modulations within these planes indicate that there is some correlation between the *z* positions of guests in adjacent tunnels.

There is no diffuse plane in the *hk*0 layer because this only contains information about the *projection* of the real space structure on the *a–b* plane in which the guests appear as a regular two-dimensional array, and the disorder in the perpendicular direction is lost. In the *hk*0 layer, therefore, the guests contribute directly to the Bragg peaks, the remaining diffuse scattering being due to the *rotational* disorder of the guests about the tunnel axis. The guests in alkane–urea and similar compounds are thought to be in approximately a trans conformation, with the plane of the molecules lying in any of six energetically favorable orientations parallel to the $1\bar{1}0$ and equivalent directions (4). The *hk*0 diffuse scattering is highly structured and is consistent with local ordering of these guest orientations into a herringbone arrangement like that of the low-temperature phase (Fig. 2) (5).

Broad diffuse bands are observed in the 0*kl* diffraction patterns perpendicular to *c**. These have a spacing corresponding to the C–C atomic separation of an alkane chain, suggesting that these diffuse features arise from disorder within the guest molecules (6).

In addition to the diffuse scattering features described above, sharp Bragg peaks additional to the urea host reflections are often observed in urea inclusion compounds. These are usually commensurate with the host reflections in the *a** and *b** directions and commensurate with the guest c_g^* repeat of the diffuse planes in the perpendicular direction. This indicates that in some regions of the crystal the guests are three-dimensionally ordered in layers perpendicular to the *c* axis (2).

In other cases a different kind of guest ordering is observed in which there is a displacement, Δ_g, in the *z* direction between guests in adjacent tunnels (Fig. 1, upper right). This gives a triclinic cell for the guest structure and the resultant scattering pattern shows characteristic hexagonal groups of peaks in the hkn_g layers arranged around the positions of the Bragg peaks of the *hk*0 layer (3, 7). Figure 1 shows schematically both types of guest ordering along with the characteristic diffraction patterns in the first diffuse layer.

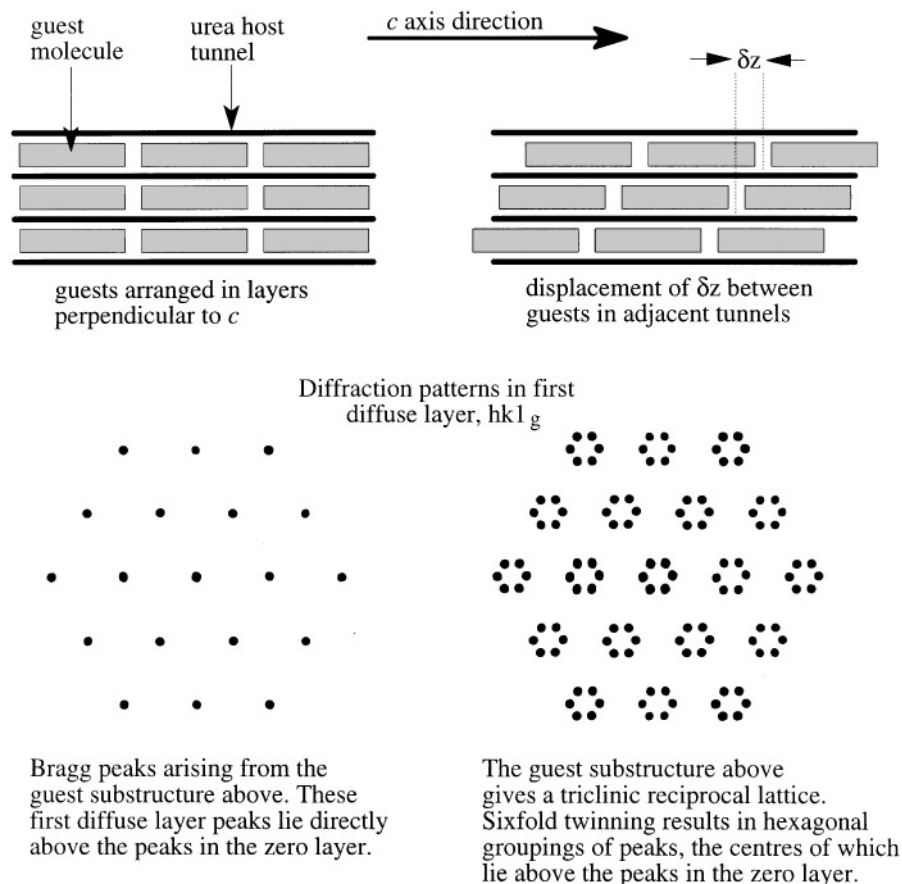[1]To whom correspondence should be addressed.

FIG. 1. Schematic drawing of two different types of guest ordering and the resulting diffraction pattern in the first diffuse layer.

In either case, the guest c-axis repeat C_g is generally incommensurate with that of the host, c_h, so that the host and guests lie on two interpenetrating incommensurate substructures, giving rise to a so-called composite modulated structure. In such cases, modulation of each substructure by the other might be expected to give rise to satellite reflections in addition to the parent Bragg reflections of each substructure, and it is surprising therefore that such satellites have so rarely been observed. In fact, they have only been observed at very low temperatures (32 K) in n-hexadecane–urea and n-nonadecane–urea (8, 9).
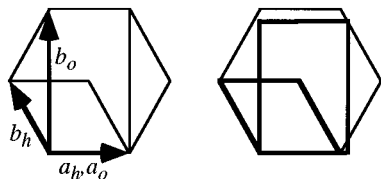

FIG. 2. Left: Relationship between hexagonal host cell parameters a_h and b_h and the undistorted orthorhombic cell parameters, a_o and b_o. Right: Distortion of orthorhombic cell observed as temperature is reduced (scale exaggerated for clarity).

More recently, large commensurate superstructures of urea inclusion compounds with bis(methyl ketone)s have been reported. In these structures, very long c-axis lengths are typically observed which correspond to n repeats of the urea host and m guest repeats (where n and m are integers). A crystal structure obtained for one of the series (octanedione–urea) indicates that the guests are tethered in place to the host structure by hydrogen bonding to urea molecules in the host tunnel walls (10, 11).

1.2. Low-Temperature Phase (III)

A low-temperature phase transition arising from ordering of the guest orientations is known to occur in alkane–urea and other urea inclusion compounds. This transition is characterized by a change from a hexagonal to an orthorhombic cell, with the guests oriented in a herringbone pattern as viewed in projection down c (12, 13). The orthorhombic cell has lattice parameters of $a_0 \approx a_h$ and $b_0 \approx 2b_h + a_h$. Figure 2 shows the orthorhombic cell and its relationship with the room temperature hexagonal cell of the host.

This phase transition is thought to be driven largely by guest–host interactions (14), with the reorientation of the guest molecules resulting in an orthorhombic distortion of the cell parameters. Since the orthorhombic cell can occur in any of three orientations with respect to the host, the resultant diffraction pattern shows peak splitting arising from the superimposed peaks of the different domains, although in reality the peak splitting is a little more complicated, indicating slightly misaligned pairs of domains in each of the three directions (4). Despite the peak overlap, systematic absences of the odd *h*00 and 0*k*0 peaks are observed in the *hk*0 diffraction pattern, and it is this that indicates the *n*-glide in the guest ordering pattern (Fig. 2).

1.3. Size Limitations of Guests

While a wide range of guests are known to form inclusion compounds with urea, the space limitations of the host tunnels, which are about 5 Å in diameter, place restrictions on the width of the included molecules. Fetterly (1) describes the limitations of guest molecules and remarks that while some molecules with bulky and/or side groups will not form urea adducts, long alkane chains can act to stabilize such groups within the urea host (1). For instance, 1-phenyloctadecane readily forms a urea inclusion compound whereas shorter molecules with a terminal phenyl group do not.

In the work described here we examine a series of *p*-di-*n*-alkylbenzene guests in which the bulky benzene ring is stabilized by an alkane on either side. We determine the limits of the series for inclusion into urea and examine the effects of incorporating a bulky group in the resulting inclusion structures at both room temperature and low temperature.

2. EXPERIMENTAL

2.1. Synthesis of p-Dialkylbenzenes

The following instruments were used: Varian VXR-300S and Varian Gemini 300 (^{1}H NMR, ^{13}C NMR at 75.43 MHz) and VG AutoSpec (mass spectra at 70 eV). The compounds 1,4-dihexylbenzene (15), 1,4-diheptylbenzene (16) and 1,4-dioctylbenzene (15) were prepared by reported procedures. Organic solvents of reagent grade were dried by published procedures (17) and distilled under nitrogen. All reactions were carried out under nitrogen by standard Schlenk techniques. Elemental analyses were carried out in-house.

Preparations: 1,4-dipentylbenzene. Pentylmagnesium bromide was prepared by adding 1-bromopentane (25.5 g, 0.17 M) dropwise to magnesium in ether (100 mL). The mixture was heated to reflux for 30 min. This Grignard reagent was added dropwise to 1,4-dichlorobenzene (9.9 g, 0.067 M) and dichloro[1,3-(diphenylphosphino)propane] nickel(II) (89 mg, 0.164 mmol) in dry, degassed ether

(100 mL) at 0°C. The reaction was allowed to warm to room temperature and then brought to reflux with stirring for 16 h. The reaction was cooled to room temperature and then quenched with water (100 mL). The reaction mixture was then extracted with ether (2×100 mL). The combined ether extracts were washed successively with water, aqueous saturated sodium bicarbonate, and again with water and then dried over anhydrous magnesium sulfate. After evaporation of the solvent the residue was distilled under reduced pressure to give a forerun of 1-chloro-4-pentylbenzene and 1,4-dipentylbenzene (1.02 g; ^{1}H NMR showed this to be ca. 92% 1,4-dipentylbenzene) (bp 112–114°C, 5.0 Torr) followed by pure 1,4-dipentylbenzene (5.09 g, 35%) (bp 114–116°C, 5.0 Torr). ^{1}H NMR (CD$_2$Cl$_2$) δ 7.35 (s, 4H), 2.85 (t, $J = 7.65$ Hz, 4H), 1.88 (m, 4H), 1.63 (m, 8H), 1.20 (t, $J = 6.90$ Hz, 6H). ^{13}C{^{1}H} NMR (CD$_2$Cl$_2$) δ 140.81, 129.02, 36.44, 32.53, 32.30, 23.51, 17.76. Anal. Calcd for C$_{16}$H$_{26}$: C, 88.00; H, 12.00. Found: C, 87.85; H, 12.20. MS (EI) *m/z* (rel int, %) 218 (M$^+$, 57), 161 (100), 105 (20), 91 (39).

The following compounds were prepared similarly from the appropriate alkyl bromide; distillation [bp (°C)/Torr] or crystallization conditions and yields are in parentheses. (1,4-Dinonylbenzene (206–208/3.0, 78%): ^{1}H NMR (CDCl$_3$) δ 7.09 (s, 4H), 2.57 (t, $J = 7.80$ Hz, 4H), 1.60 (t, $J = 6.93$ Hz, 4H), 1.27 (broad s, 24H), 0.90 (t, $J = 6.93$ Hz, 6H); lit. (18) ^{1}H NMR (CCl$_4$) δ 6.95 (s, 4H), 2.52 (t, $J = 7$ Hz, 4H), 1.27 (broad s, 28H), 0.90 (t, $J = 7$ Hz, 6H); ^{13}C{^{1}H} NMR (CDCl$_3$) δ 140.08, 128.22, 35.61, 31.94, 31.66, 29.61, 29.58, 29.44, 29.38, 22.72, 14.15. Anal. Calcd for C$_{24}$H$_{42}$: C, 87.19; H, 12.81. Found: C, 87.49; H, 12.94. MS (EI) *m/z* (rel int, %) 330 (M$^+$, 94), 217 (27), 105 (100). 1,4-Didecylbenzene (crystallized from *n*-pentane at -20°C, 70%): ^{1}H NMR (CD$_2$Cl$_2$) δ 7.35 (s, 4H), 2.87 (m, 4H), 1.92 (m, 4H), 1.62 (m, 28H), 1.23 (m, 6H); ^{13}C{^{1}H} NMR (CD$_2$Cl$_2$) δ 140.91, 129.24, 36.84, 33.24, 32.93, 31.10, 30.99, 30.90, 30.82, 30.71, 23.97, 15.17. Anal. Calcd for C$_{26}$H$_{46}$: C, 87.07; H, 12.93. Found: C, 86.85; H, 13.08. MS (EI) *m/z* (rel int, %) 358 (M$^+$, 81), 105 (100); MS (EI) *m/z* (parent ion) calcd for ^{12}C$_{26}$^{1}H$_{46}$ 358.3600, found 358.3588.

2.2. Growth of Urea Inclusion Compounds

Crystals of the inclusion compounds were grown by evaporation from a solution of 1 g of urea: 0.5 g of guest in propanol, which represents an excess of guest with respect to the expected proportion of each guest in an inclusion compound. Attempts to grow crystals were made with six of the *p*-dialkylbenzene series from *p*-dipentylbenzene to *p*-didecylbenzene. Inclusion compounds formed readily for all the guests except *p*-dipentylbenzene and *p*-dihexylbenzene; the former did not form an inclusion compound, and the latter gave a mixture of crystals, most of which turned out to be urea, while the remainder were crystals of the inclusion compound.

The crystals of all five inclusion compounds grew as needles up to 5 mm in length and 0.5 mm in diameter, with a hexagonal cross section. Many of the crystals had a characteristic flaw of a fine hollow tube down the center.

2.3. X-Ray Diffuse Scattering Experiments

X-ray diffuse scattering measurements were recorded using the position-sensitive detector (PSD) diffractometer system described by Osborn and Welberry (19). This system uses a flat-cone Weissenberg geometry and permits measurement of the X-ray scattering in layers of reciprocal space perpendicular to the rotation axis of the crystal.

For each compound crystals were mounted parallel to both c and a so that diffuse scattering measurements could be made of the $hk0$ and $0kl$ sections, respectively. The crystals were aligned by observation of reflected light from the crystal faces using the Stoe telescope and then checked with oscillation photographs. Following alignment of the crystals mounted parallel to a^*, it was necessary to grind the crystals to produce a more isotropic cross section using the crystal lathe described by Wood $et\ al.$ (20).

Measurements of the $hk0$ and $0kl$ layers were made at room temperature and at 120 K using an Oxford Cryostream for cooling.

3. RESULTS AND DISCUSSION

All the samples examined showed many features characteristic of urea inclusion compounds such as sharp planes of diffuse scattering perpendicular to c^* (the first three layers are indicated as d1, d2, and d3 on Figs. 4–8c) and diffuse scattering in the $hk0$ layer arising from orientational disorder of the guests (typically butterfly and X-shaped diffuse streaks such as those highlighted as B and X in Fig. 4a). However, they also showed superstructure peaks and unusual low-temperature behavior that appear to be unique to this series. These are described and discussed in detail in the following and are summarized in Table 1.

3.1. Dihexylbenzene

Room temperature. The scattering pattern in the $hk0$ layer (Fig. 4a) showed diffuse features (marked B and X) typical of urea inclusion compounds, indicating that orientational disorder of the guests is an important feature of the structure. The Bragg peaks, however, indicated an apparently hexagonal cell with doubled a and b axes (≈ 16.4 Å) with respect to the structure of the urea host.

The $0kl$ pattern (Fig. 4c) showed the diffuse planes characteristic of urea inclusion compounds although the planes with odd l_g (e.g., d1 and d3) were much stronger in intensity than the even l_g planes. Additional Bragg peaks along the c axis indicated a doubling of the host c axis (≈ 22 Å) and

were approximately commensurate with the diffuse planes. Satellite peaks were also observed extending in the direction of the c^* axis on either side of the Bragg peaks, indicating a modulation with a wavelength of approximately 420 Å. A magnified view of these barely resolved satellites, taken from the original Weissenberg-format data, is shown as an inset to Fig. 4c.

If we ignore the weak satellites, the parent reflections indicate an apparent doubling of all three axes due to the formation of a three-dimensional superstructure, arising from orientational ordering of the guests and interchannel longitudinal ordering. This relatively small cell precludes a truly ordered structure with hexagonal symmetry; however, this still leaves a number of lower symmetry cells which could give rise to this diffraction pattern, provided there was no accompanying metrical strain distortion associated with the lower symmetry. One possibility is a cell with lattice parameters of $a = b = 2a_h$ and $\gamma = 120°$ with respect to the a_h and b_h cell parameters of the host. Such a cell could have monoclinic symmetry or hexagonal symmetry (provided one in four of the guests was disordered) or could be the primitive cell of a C-centered orthorhombic system with lattice parameters of $2a_h$ and $4b_h + 2a_h$. The lower symmetry cells could have three possible orientations with respect to the host, and multiple domains of each orientation within the crystal would still give rise to a diffraction pattern of hexagonal symmetry. A second possible cell has lattice parameters a_h and $2b_h + a_h$, similar to that of the low-temperature phase of other urea compounds, but with metrically hexagonal geometry. Once again, threefold twinning of domains of three different orientations would give rise to a hexagonal diffraction pattern like that observed.

The satellite peaks extending in the c^* direction from the Bragg peaks indicate a structural modulation which is likely to arise from a slight mismatch between the repeat distance of the guests and the doubled c axis. It can be seen from the diffraction pattern that the diffuse planes are slightly more widely spaced than the Bragg layers perpendicular to c^*. Therefore, considering the three-dimensional ordering solely in terms of a $2 \times 2 \times 2$ superstructure of the urea host is only an approximation. The satellite peaks in the $0kl$ pattern are strongest for peaks with odd k, which primarily arise from scattering by the guests. The structure could therefore be described as two interpenetrating substructures of host and guest, respectively, in which the guest substructure is more heavily modulated by the host than the reverse.

Low temperature (120 K). Both $hk0$ and $0kl$ diffraction patterns (Figs. 4b and 4d, respectively) are considerably different from their room temperature equivalents and indicate a phase transition accompanied by a distortion of the cell parameters away from hexagonal values. The $hk0$ diffuse scattering and the diffuse planes perpendicular to c^*
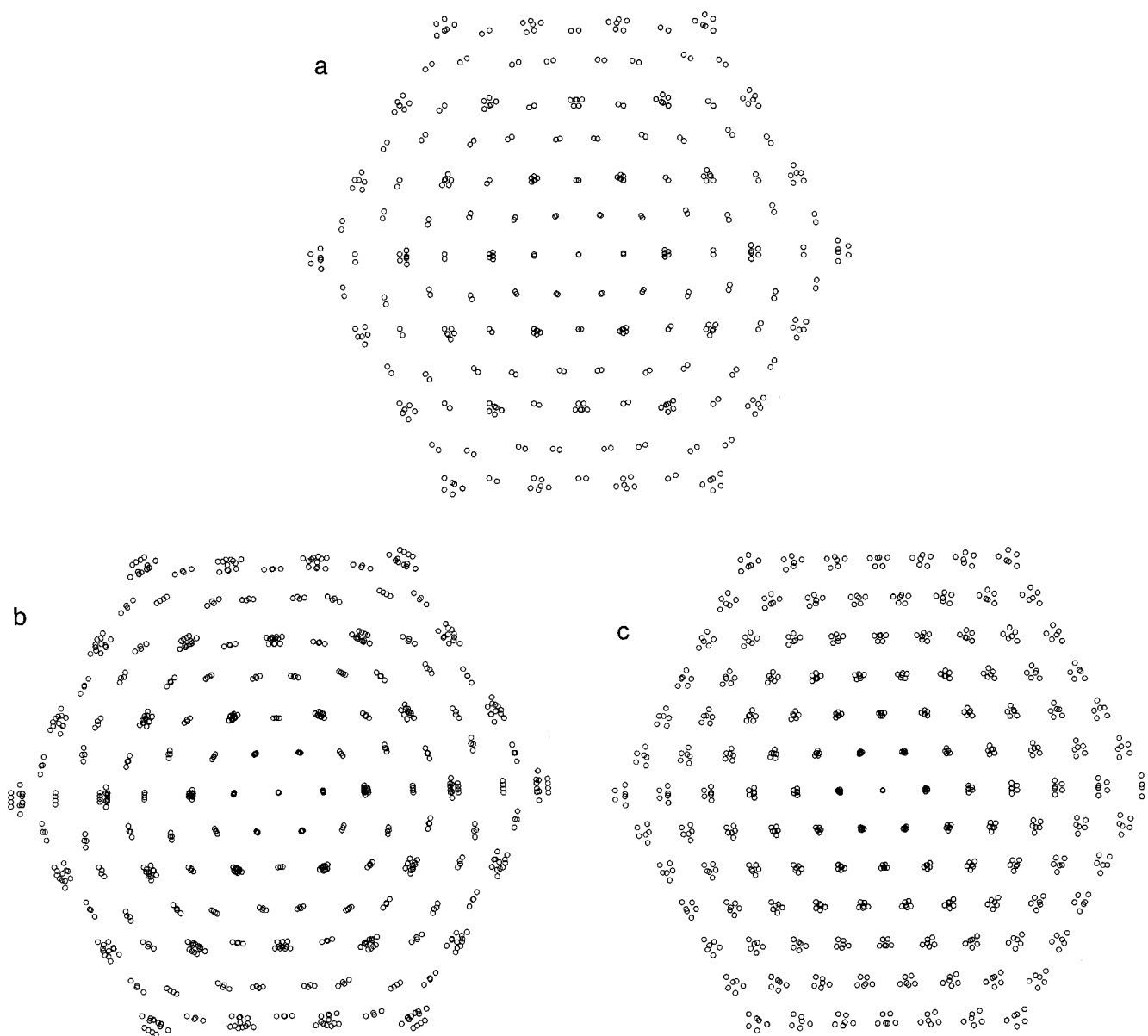
FIG. 3. Peak splitting for an orthorhombic cell with lattice parameters of approximately a_h and $2b_h + a_h$. (b) Peak splitting for a small monoclinic distortion of the orthorhombic cell in (a). (c) Peak splitting for cell of $a = b \approx 2a_h$, $\gamma \neq 120°$.

have almost disappeared, peak splitting in the direction perpendicular to the c^* axis is observed, and the satellite peaks are no longer visible in the $0kl$ pattern, leaving only the doubled c-axis peaks. The disappearance of the diffuse scattering and the satellites indicates a change to a more ordered structure in which the guests have become locked into the host structure along the c direction to form a truly commensurate superstructure.

The peak splitting in the $hk0$ layer is particularly interesting as it cannot arise from an orthorhombic cell like that of the low-temperature phase of the alkane–urea inclusion compounds. For such a cell, only peaks corresponding to the urea host substructure ($h = 2n$, $k = 2n$, for n integer) are split in 2θ as well as ω (see Fig. 3a), whereas in the observed $hk0$ diffraction pattern, all the peaks are split in 2θ. Three nonhost peaks showing 2θ splitting are highlighted in Fig. 4b. This splitting could be generated either by a slight monoclinic distortion of the orthorhombic cell with cell parameters of $\approx a_h$ and $\approx 2a_h + b_h$ (Fig. 3b) or by a cell with parameters of $a = b \approx 2a_h$ (Fig. 3c). The split peaks are resolved in the 2θ direction but show streaking in the ω direction, indicating strain between slightly misoriented domains. The existence of such domains has been demonstrated in orthorhombic low-temperature phases by (4).
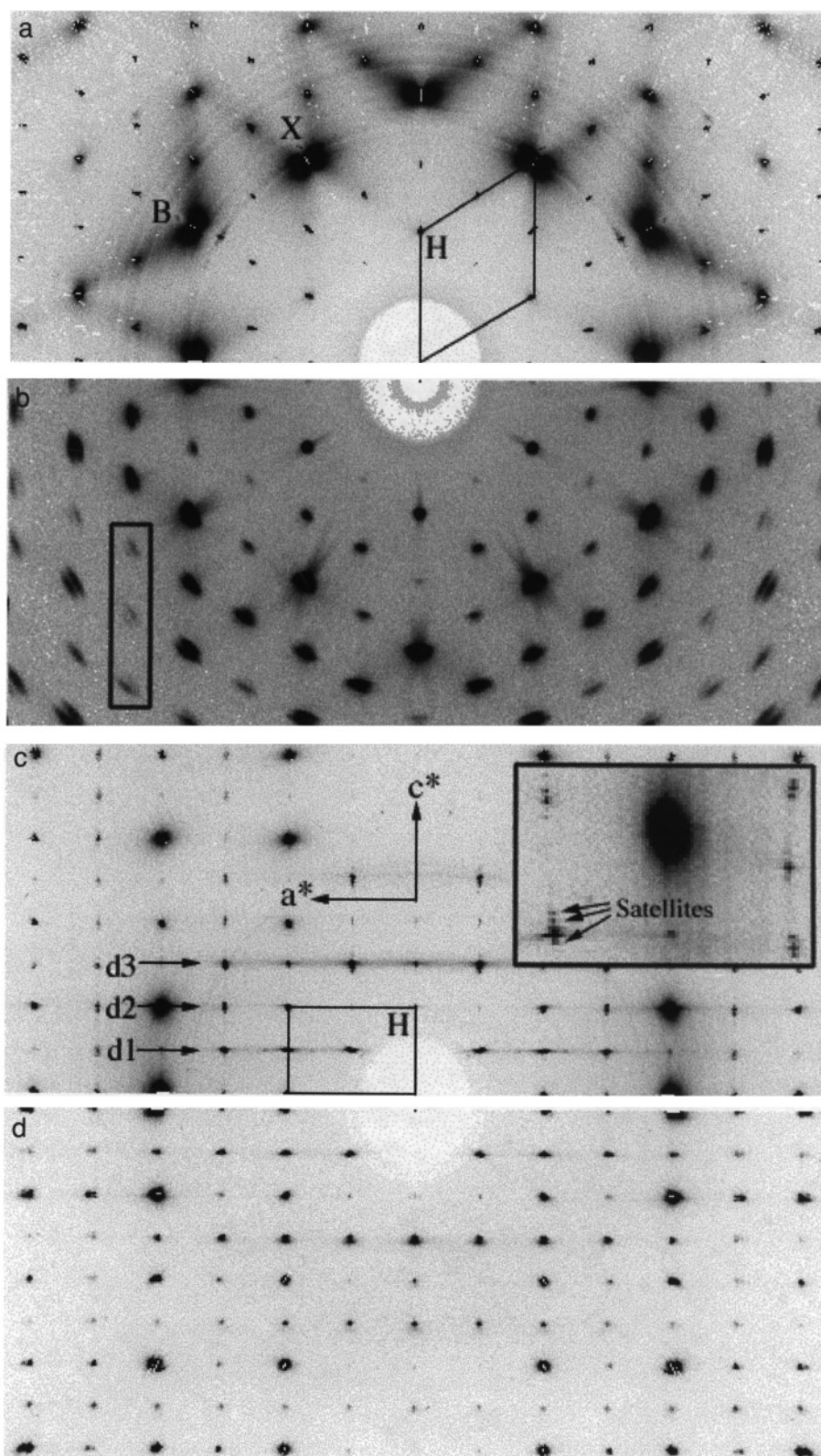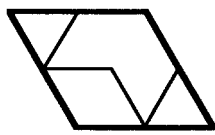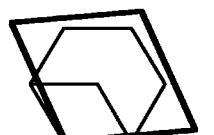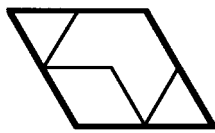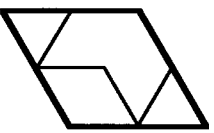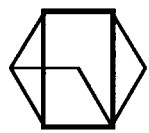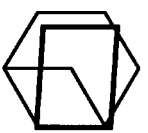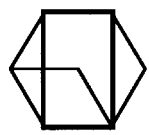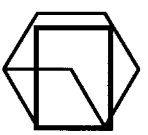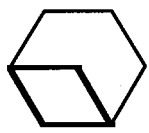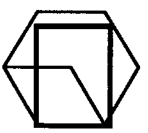
FIG. 4. Dihexylbenzene–urea diffraction patterns. (a) $hk0$ layer, 290 K. Characteristic butterfly and X-shaped diffuse features arising from rotational disorder of guests are marked B and X, respectively. Reciprocal lattice of urea host is marked H. (b) $hk0$ layer, 120 K. Peak splitting in peaks where $h, k = 2n + 1$ is highlighted in box. (c) $0kl$ layer, 290 K. First three diffuse planes are marked d1, d2, and d3. Satellite peaks are magnified in inset. Reciprocal lattice of urea host is marked H. (d) $0kl$ layer, 120 K. A much reduced diffuse scattering is evident.

TABLE 1
Summary of Cell Dimensions for the Five Compounds at Room Temperature and 120 K

Compound	c axis length	Likely room temperature cell	Likely low temperature cell	Percentage distortion of cell at 120K*	Cell parameters at 120K relative to room temp host cell.†
Dihexylbenzene/ urea	$2c_h=22.02$Å (plus ~420Å modulation at room temp)			1.9%	$a=b=1.962a_h$ $\gamma=118.7°$
Diheptylbenzene/ urea	$13c_h\approx143$Å			0%	$a=b=1.990a_h$ $\gamma=120°$
Dioctylbenzene/ urea	$19c_h\approx209$Å			2.2%	$a=0.998a_h$ $b=(0.970)x(2b_h+a_h)$ $\gamma>90°$
Dinonylbenzene/ urea	$21c_h\approx231$Å			2.9%	$a=1.005a_h$ $b=(0.966)x(2b_h+a_h)$ $\gamma=90°$
Didecylbenzene/ urea	$c_h=11.01$Å (plus ~130Å modulation at low temperature)			2.9%	$a=1.006a_h$ $b=(0.966)x(2b_h+a_h)$ $\gamma=90°$

*Change in ratio of ortho-hexagonal a and b axes between room temperature and 120 K.
†Cell parameters assuming that proposed cell is correct.

Figures 3b and 3c show the peak splitting expected for the two possible low-temperature cells already described. In Fig. 3b, which is for a monoclinic distortion of the orthorhombic low-temperature cell ($a \approx a_h$, $b \approx 2a_h + b_h$), all the peaks show splitting in 2θ, although the splitting of the $h, k = 2n$ peaks in 2θ is larger than that of other peaks. In addition, the peaks lying on mirror planes of the pattern have a more complex splitting in 2θ than the twofold splitting seen in the orthorhombic phase shown in Fig. 3a. The greater the departure from orthorhombic symmetry, the greater the 2θ splitting in the peaks with odd h and k indices and the more complex the splitting in the peaks with even h and k indices.

Figure 3c shows the splitting expected for a cell with lattice parameters of $a = b \approx 2a_h$ and $\beta > 120°$. This cell could be monoclinic or the primitive cell of a C-centered orthorhombic system, although this particular distortion (in which $a = b$) would be more characteristic of an orthorhombic system. Unlike the pattern in Fig. 3b, the peaks lying on mirror planes show only twofold splitting in 2θ,

and the splitting of peaks with odd h and k indices is of the same magnitude as that of the peaks where $h, k = 2n$. This pattern shows greatest similarity to that observed in the low-temperature phase of dihexylbenzene–urea, making this the most likely cell for the low-temperature phase.

Since orientational ordering of the guests is already present at room temperature, the phase transition is likely to be a change from a metrically hexagonal to a distorted cell rather than a reorientation of the guests. This suggests that the room temperature cell is the metrically hexagonal equivalent of the low-temperature cell described, which as mentioned previously, could be either monoclinic or C-centered orthorhombic. This experiment cannot determine whether the c-axis ordering (i.e., loss of satellites and diffuse scattering) occurs at the same time as the cell-distortion transition or as a separate phase transition; however, differential scanning calorimetry indicated only one phase transition between room temperature and ~ 140 K occurring at 257 K.

3.2. Diheptylbenzene

Room temperature. Like dihexylbenzene–urea the $hk0$ diffraction pattern (Fig. 5a) of diheptylbenzene indicated apparently doubled a and b axes with respect to the urea host. This again could correspond to a hexagonal, mono-clinic, or C-centered orthorhombic primitive cell ($a = 2a_h$ and $b = 2b_h$) or an orthorhombic or monoclinic cell ($a = a_h$ and $b = 2b_h + a_h$) and is a consequence of orientational ordering of the guests. In contrast to dihexylbenzene–urea, the $0kl$ pattern (Fig. 5c) showed a 13-fold increase in the length of the c axis with respect to the urea host, giving a lattice parameter of $13 \times c_h \approx 143$ Å. This is equal to the length of six of the guest molecules, as could be verified by the coincidence of the diffuse planes (corresponding to a single guest repeat) with the $l = 6n$ layers.

The continuity of the Bragg peaks along the c^* axis indicates that this is a fully commensurate 13-fold super-structure in the c direction (with respect to the urea host) rather than a modulated structure like dihexylbenzene–urea. The guest molecules are separated by $2\frac{1}{6}$ times the length of the host c-axis repeat along the host tunnels, which means that the host environment for each guest is related to the previous one by a 6_1 screw. Hence the 6_1 screw of the host is likely to be preserved in the superstructure, as can be verified from the $00l$ systematic absences. Hence the correct cell is a hexagonal cell with cell parameters $2a_h$, $2b_h$, and $13c_h$ with respect to the host substructure. Since the guests have 2-fold symmetry, it is probable that they would sit on the 2-fold axes of the host, in which case the superstructure would have the same $P6_122$ space group as the host. This compound is the only one of those examined for which this coincidence of symmetry occurs, and it should be noted that the diffuse planes are weaker and the superstructure peaks along the c axis are stronger than in the other materials examined, which parallels observations by Hollingsworth *et al.* (11) of alkanedione–urea inclusion superstructures.

Both the $hk0$ and $0kl$ diffraction patterns show diffuse scattering features. The $hk0$ diffuse scattering is like that of many other urea inclusion compounds and indicates that orientational disorder is still a feature of this material. The diffuse planes in the $0kl$ layer were much weaker than in other inclusion materials, as might be expected from the high degree of guest ordering along the c axis, and only layers corresponding to odd l_g (e.g., d1 and d3) were visible.

Low temperature (120 K). The low-temperature $hk0$ (Fig. 5b) diffraction pattern was not markedly different from that at room temperature although the Bragg peaks appeared to be slightly broadened, possibly indicating some peak split-ting. However, separate peaks could not be resolved. The $0kl$ pattern (Fig. 5d) clearly showed that the 6_1 screw had been broken with the appearance of additional peaks other than $k = 6n$ along the c^* axis (e.g., the peak marked E in Fig.

5d). A phase transition to lower symmetry is indicated but with only a slight effect (if any) on the lattice parameters.

Diffuse features arising from rotational disorder of the guests were still visible in the $hk0$ pattern although they more closely resembled the type of diffuse features seen in alkane–urea inclusion compounds just above the phase transition with diffuse intensity concentrated in blobs be-tween the peaks of the host substructure. These changes in the diffuse scattering pattern indicate an increase in the correlation length of the short-range ordering in the dis-ordered regions of the crystal.

3.3. Dioctylbenzene

Room temperature. Once again the $hk0$ diffraction pat-tern (Fig. 6a) showed additional Bragg peaks consistent with an apparent doubling of the a and b axes with respect to the urea host. The Weissenberg diffraction data revealed that the room temperature cell was geometrically hexagonal but because the stationary counting method makes it diffi-cult to ascertain true symmetry, additional measurements of Bragg peak intensities were made on a four-circle diffrac-tometer. From these measurements $6mmm$ Laue symmetry was confirmed. The $hk0$ diffuse scattering, arising from regions with rotationally disordered guests, was also quite strong, indicating that despite the ordering of the guest molecules relative to the completely disordered urea inclu-sion compounds, disorder is still an important feature of the structure.

The $0kl$ diffraction pattern (Fig. 6c) showed diffuse layers, indicating the presence of some longitudinal disorder, and also Bragg peaks consistent with a 19-fold increase in the length of the c axis (these peaks could only be fully resolved in the Weissenberg-format raw data). This corresponds to the length of eight guest molecules (≈ 209 Å). Clearly the ratio of guest to host in this case does not permit the preservation of the hexagonal symmetry with a fully ordered structure. The relative weakness of the superstructure peaks in this inclusion compound as compared to those of dihep-tylbenzene–urea reflects the lack of such a well-defined symmetrical relationship between guest and host.

The possibilities for the superstructure cell in this case are the same as those for dihexylbenzene: a cell with lattice parameters of $a = b = 2a_h$ which could have hexagonal symmetry with some disordering of the guests, or otherwise monoclinic or orthorhombic (as the primitive cell of a C-centered system) symmetry. The other possible cell is orthorhombic with lattice parameters of $a = a_h$ and $b = 2b_h + a_h$.

Low temperature (120 K). The low-temperature patterns (Figs. 6b and 6d) showed a marked reduction in the intensity of both the diffuse planes and the $hk0$ diffuse scattering, indicating a reduction in the disorder within the structure.
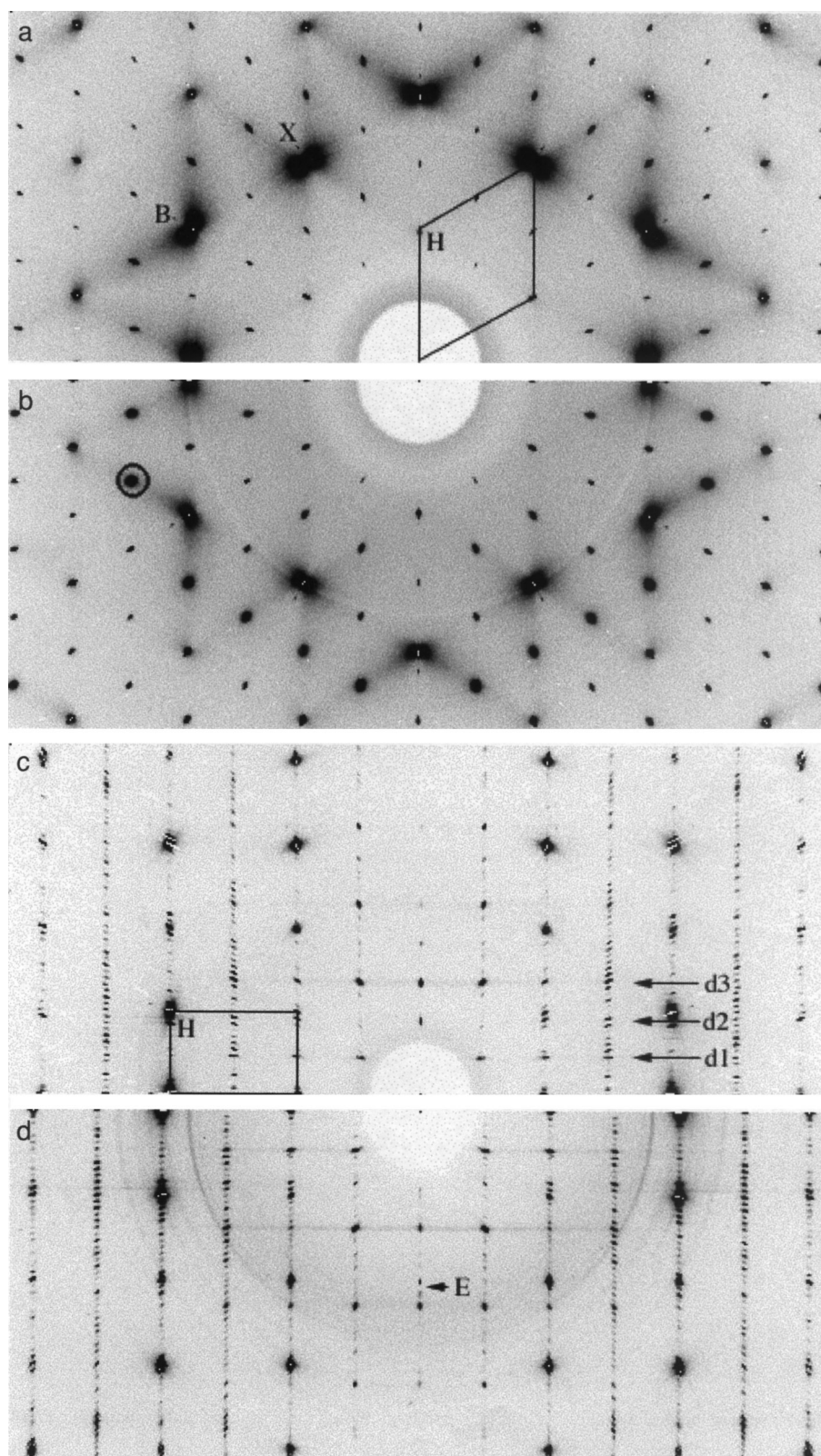
FIG. 5. Diheptylbenzene–urea diffraction patterns. (a) *hk*0 layer, 290 K. Characteristic butterfly and X-shaped diffuse features arising from rotational disorder of guests are marked B and X, respectively. Reciprocal lattice of urea host is marked H. (b) *hk*0 layer, 120 K. Diffuse "blob" is highlighted with circle. (c) 0*kl* layer, 290 K. First three diffuse planes are marked d1, d2, and d3. Reciprocal lattice of urea host is marked H. (d) 0*kl* layer, 120 K. Additional peak indicating breaking of 6_1 symmetry is marked E.
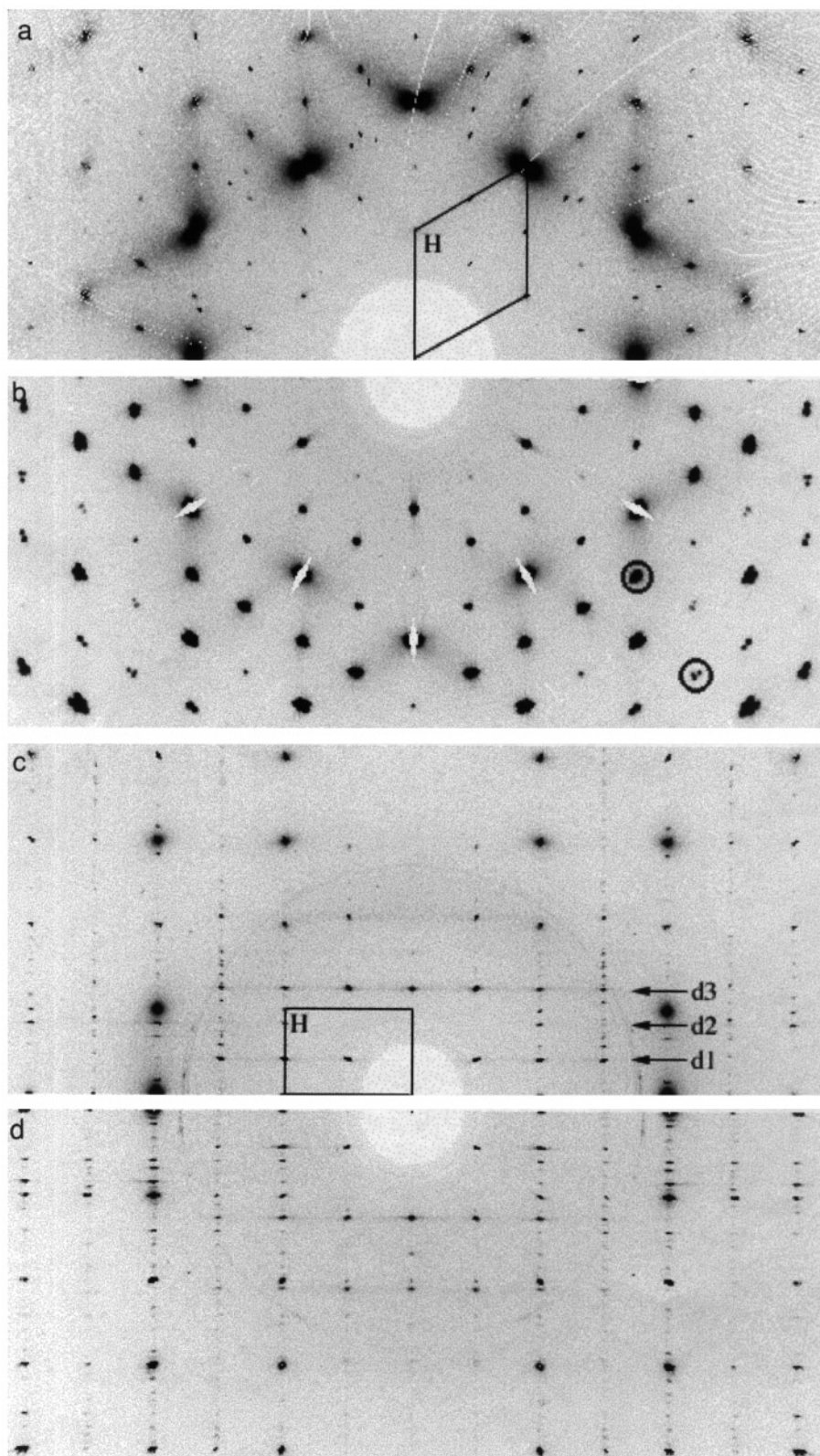
FIG. 6. Dioctylbenzene–urea diffraction patterns. (a) $hk0$ layer, 290 K. Reciprocal lattice of urea host is marked H. (b) $hk0$ layer, 120 K. Slight splitting of $h, k = 2n + 1$ peaks is highlighted with circles. White "blank" areas on the pattern arise from segments which were not measured to avoid swamping the detector with intensity from very strong Bragg peaks. (c) $0kl$ layer, 290 K. First three diffuse planes are marked d1, d2, and d3. Reciprocal lattice of urea host is marked H. (d) $0kl$ layer, 120 K.

The Bragg peaks for which $h, k = 2n$ show a large degree of splitting and there also appears to be a small degree of splitting of peaks with odd h or k indices (highlighted with circles in Fig. 6b). This is likely to arise from a small monoclinic distortion of the orthorhombic cell with parameters of $a \approx a_h$ and $b \approx 2a_h + b_h$ (see Fig. 3b). The corresponding undistorted cell is therefore the most likely cell at room temperature.

3.4. Dinonylbenzene

Room temperature. The diffraction patterns for dinonylbenzene–urea (Figs. 7a and 7c) closely resemble those of dioctylbenzene–urea at room temperature. There is still significant diffuse scattering and apparent doubling of the *a* and *b* axes with respect to those of the host. As with dioctylbenzene–urea, the peak intensities of the $hk0$ pattern do not seem to have hexagonal symmetry. In this case the superstructure peaks in the $0kl$ pattern show a 21-fold increase in the *c* axis compared to that of the host, which corresponds to the length of eight guest molecules. The possible unit cells are the same as those for dihexylbenzene–urea and dioctylbenzene–urea as the host/guest ratio does not permit a fully ordered hexagonal structure, and consequently the superstructure peaks are relatively weak.

Low temperature (120 K). The low-temperature diffraction patterns (Figs. 7b and 7d) showed peak splitting in which only peaks with $h, k = 2n$ were split in 2θ (examples highlighted with squares in Fig. 7b and marked S in Fig. 7d). This is consistent with an orthorhombic cell with parameters of $a \approx a_h$ and $b \approx 2b_h + a_h$, suggesting that the metrically hexagonal equivalent of this cell is the most likely cell at room temperature.

3.5. Didecylbenzene

Room temperature. Unlike the inclusion compounds described in the previous sections, many features of the didecylbenzene–urea $0kl$ and $hk0$ diffraction patterns (Figs. 8a and 8c) closely resembled those of urea inclusion compounds with longitudinally and rotationally disordered guests. The unit cell dimensions corresponded to those of the host, with no evidence of superstructure peaks. Blobs of diffuse intensity were noted in the $hk0$ diffraction pattern similar to those seen in alkane–urea compounds just above the phase transition to the orthorhombic phase.

The diffuse planes visible in the $0kl$ pattern, however, had unusually strong modulations of intensity. A measurement of the hkl_g diffuse scattering pattern (the first diffuse layer (Fig. 9)) showed that the bright regions were sharp circles of diffuse scattering centered on the positions of the Bragg peaks in the zero layer. These indicate noncrystallographic ordering of the disordered guests over a range of ~ 150 Å. On close examination, the circles appear to have some

structure with sixfold symmetry. This may indicate that these features are related to the hexagonal clusters of Bragg peaks seen in the first diffuse layer of urea inclusion compounds with a triclinic guest subcell (Fig. 1).

Low temperature. At 120 K the diffuse scattering has almost entirely disappeared from the $hk0$ diffraction pattern, and the Bragg peaks showed splitting of the type observed in the low-temperature phase of alkane–urea inclusion compounds. This indicates an orthorhombic cell with lattice parameters $a = a_h$ and $b = 2b_h + a_h$, with an *n*-glide perpendicular to *c*. The *n*-glide is clearly indicated by the systematic absences marked A in Fig. 8b.

Unlike the alkane–urea low-temperature phase, the $0kl$ pattern shows additional peaks along the *c** direction, which appear to indicate a repeat distance of $\approx 12c_h$. The peaks with odd *h*—which are primarily due to guest scattering—are the strongest and their intensity is strongly modulated, with the peaks becoming more intense close to the hkn_h planes containing the host substructure reflections. This is a modulated structure like that observed in dihexylbenzene–urea at room temperature rather than a superstructure as observed in the other dialkylbenzene–urea compounds. In addition, there appear to be systematic absences of the superstructure peaks where $h = 2n + 1$ and $l = 2n$, which is what would be expected for an *n*-glide. However, too few of the superstructure peaks with $h = 2n$ are visible to check for the corresponding $l = 2n + 1$ absences in these layers.

The diffuse layers perpendicular to *c** are still pronounced at low temperature and they extend further in the hkn planes. The intensity modulations within these layers are even stronger at 120 K than at room temperature.

4. SUMMARY AND CONCLUSIONS

The inclusion in the urea host of molecules containing benzene groups has resulted in a series of compounds with a range of unusual behavior. This includes the formation of superstructures of various different symmetries, different low-temperature phases, modulated structures, and structures with important local ordering features. In each case the driving factor appears to be the tight fit of the benzene ring in the narrow tunnels of the urea host. While the varied nature of this series of inclusion compounds warrants description on a compound by compound basis (Section 3), it is useful to summarize here some of the more significant observations.

4.1. Diheptylbenzene–Urea: A High-Symmetry Superstructure

As described in detail in Section 3.2, the intermolecular spacing of the guest diheptylbenzene molecules, being
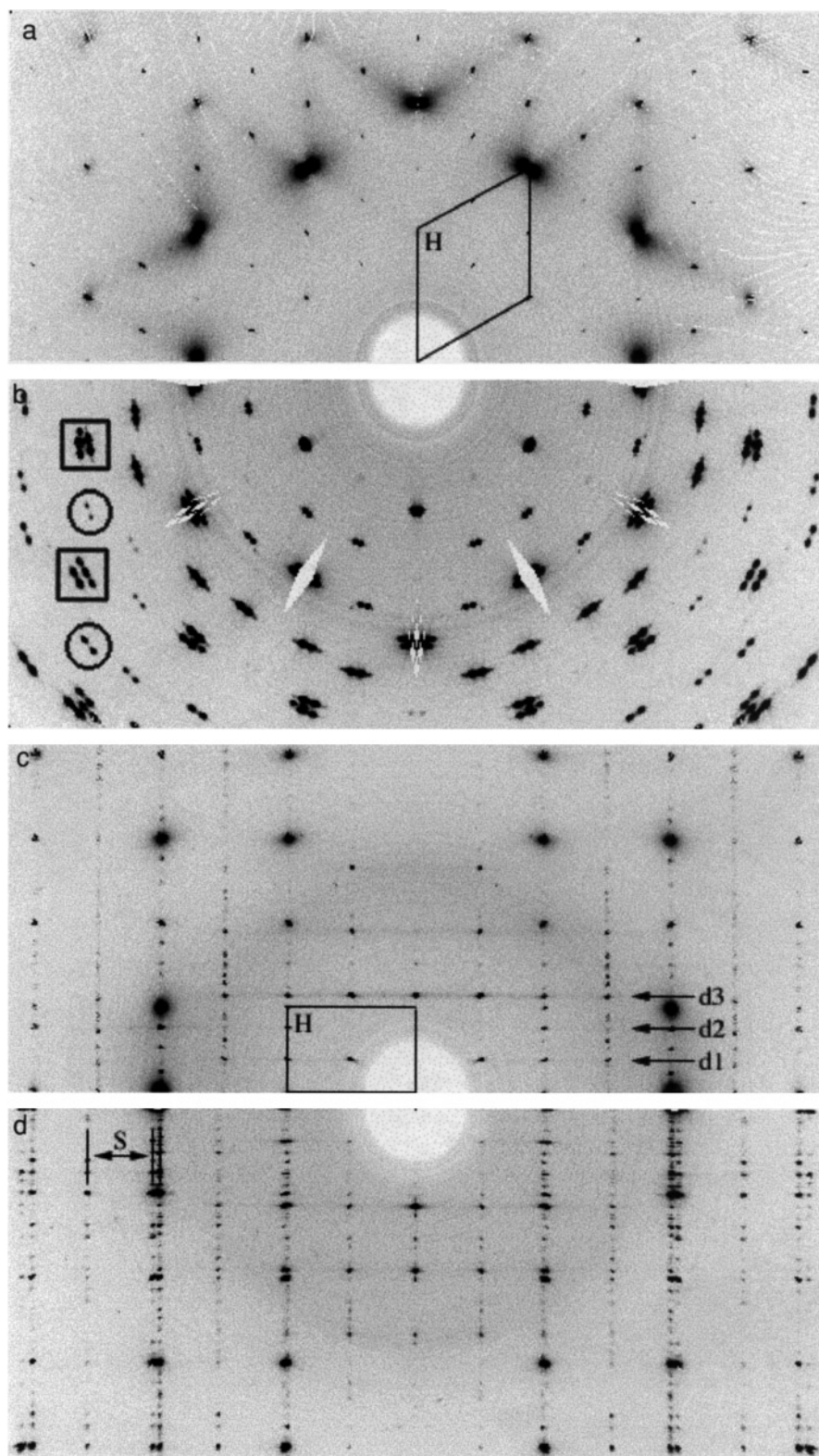
FIG. 7. Dinonylbenzene–urea diffraction patterns. (a) *hk*0 layer, 290 K. Reciprocal lattice of urea host is marked H. (b) *hk*0 layer, 120 K. Different splittings of $h, k = 2n$ and $h, k = 2n + 1$ peaks are highlighted with squares and circles, respectively. White "blank" areas on the pattern arise from segments which were not measured to avoid swamping the detector with intensity from very strong Bragg peaks. (c) 0*kl* layer, 290 K. First three diffuse planes are marked d1, d2, and d3. Reciprocal lattice of urea host is marked H. (d) 0*kl* layer, 120 K. Different splittings of even and odd *h* layers are highlighted at S.
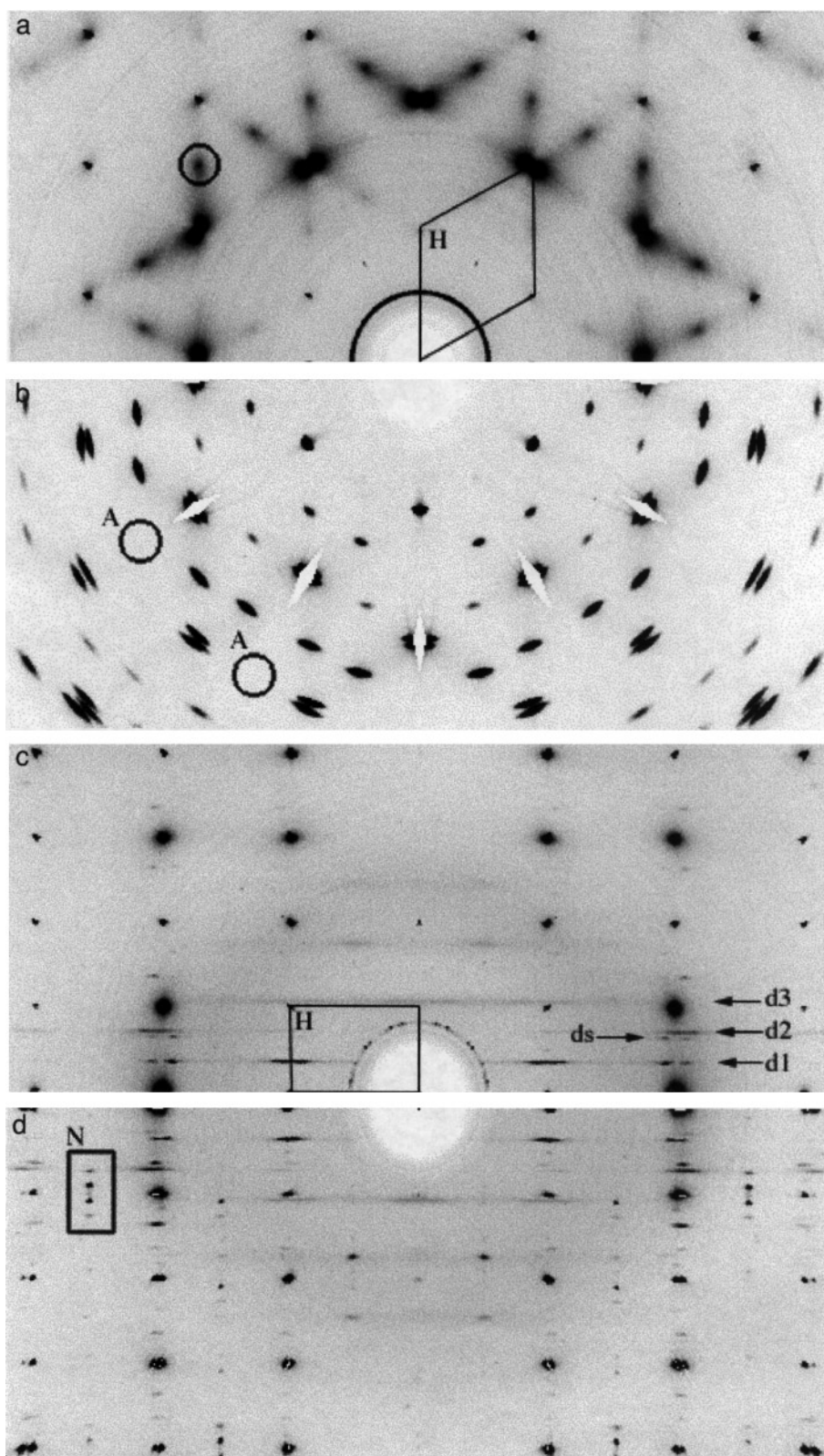
FIG. 8. Didecylbenzene–urea diffraction patterns. (a) *hk*0 layer, 290 K. Reciprocal lattice of urea host is marked H. (b) *hk*0 layer, 120 K. Systematic absences due to *n*-glide are marked A. White "blank" areas on the pattern arise from segments which were not measured to avoid swamping the detector with intensity from very strong Bragg peaks. (c) 0*kl* layer, 290 K. First three diffuse planes are marked d1, d2, and d3, and "extra" diffuse layer is marked ds. Reciprocal lattice of urea host is marked H. (d) 0*kl* layer, 120 K. A group of satellite reflections is highlighted in the box marked N.
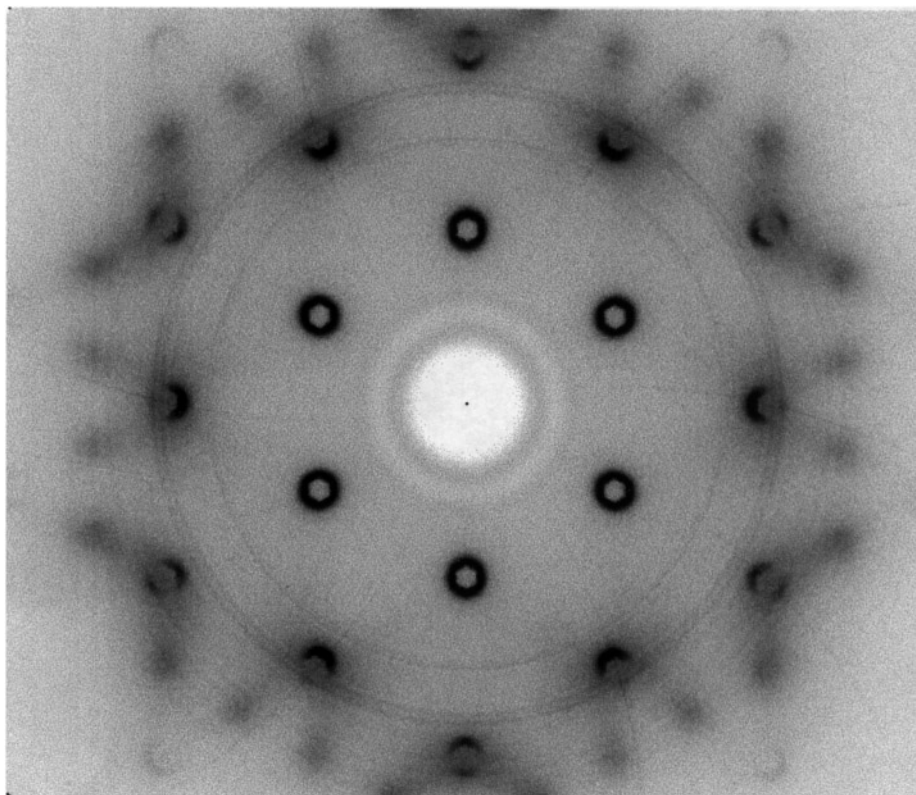
FIG. 9. Diffraction pattern of the first diffuse layer ($d1(hkl_g)$) in didecylbenzene–urea.

$2\frac{1}{6}$ times the c-axis length of the host, permits a coincidence of symmetry, resulting in the preservation of the 6_1 axis (paralleling similar observations in other inclusion compounds by Hollingsworth *et al.* (11)). It is likely in fact that the superstructure has the full 6_122 symmetry of the host.

As the structure is hexagonal, it is a suitable candidate for a single-crystal structure determination, both because it is the most highly ordered of the superstructures observed and hence has stronger superstructure peaks and because it will not be twinned. Such a structure determination would provide considerable insight into the conformation of alkanes in a urea host. This is a subject of considerable interest and debate (21–23), but the disorder of the guests in the majority of urea inclusion compounds normally rules out conventional X-ray crystal structure determination as a viable tool. The large cell of diheptylbenzene–urea (particularly the 143-Å c axis) presents a challenge in terms of conventional X-ray data collection and requires the use of image plate or CCD techniques more commonly used with protein crystals. Work in this area is ongoing.

4.2. Structural Modulation in Dihexylbenzene

The observation of incommensurate satellite peaks, corresponding to a modulation wavelength along c of ~ 420 Å, in dihexylbenzene–urea at room temperature is particularly interesting, as such peaks have previously been observed in urea inclusion compounds only at very low temperatures (20–30 K). The observation of these peaks is an indication of the strains placed on the structure by the need to accommodate the benzene ring of the guest molecule in the narrow urea tunnels.

In dihexylbenzene–urea it is only a slight mismatch between the superstructure c-axis repeat and the natural molecular separation of the dihexylbenzene molecules (indicated by the diffuse planes) that results in the modulation. If the mismatch had been larger, a long-range commensurate superstructure might have formed, like those observed in the diheptyl, dioctyl, and dinonylbenzene inclusion compounds described.

4.3. "Local" Order in Didecylbenzene–Urea

The sharpness of the diffuse circles observed in the first diffuse layer of didecylbenzene–urea indicates "local" ordering with a scale length of around 150 Å. This shows that even when the guest molecules are sufficiently long (and the benzene rings sufficiently separated) that a superstructure does not form, the disposition of the benzene rings within the structure is still strongly affecting the local organization of the guest molecules.

A more detailed analysis of the diffuse scattering in this compound would give a clearer picture of the local ordering scheme and in particular would indicate if it has anything in common with the triclinic (long range) guest ordering observed in some other urea inclusion compounds (3, 7). It would be particularly interesting to see if the same diffuse features occur in urea inclusion compounds with longer dialkylbenzene guests. It may be that the scale length of any local ordering would be reduced as the guests become longer and the tendency for the benzene rings of guests in adjacent tunnels to impinge on one another decreased. Further work in this direction is planned.

4.4. Orientational Ordering and Superstructure in the a–b Plane

The formation of superstructures in the *a–b* plane is in part reminiscent of the low-temperature phase in other urea compounds, arising as it does from an orientational ordering of the guests. However, these superstructures do not have an *n*-glide like the low-temperature phase of other urea inclusion compounds, but the fact that they form at room temperature is another indication of the constraints placed on the structures by the size of the guest's benzene ring.

4.5. Conclusion

Incorporation of guests containing a benzene ring into the urea host has clearly affected the resulting inclusion structures. Unlike the large urea inclusion superstructures observed by Hollingsworth *et al.* (11), in which hydrogen bonding between guests and the host is the controlling factor, these superstructures result entirely from the bulkiness of the benzene ring within the host. The benzene rings produce a "bulge" in the tunnel walls, and organization of both orientation and longitudinal position of guests in adjacent tunnels would seem to be necessary to reduce the resulting strain. This accounts for a number of observations. Dipentylbenzene does not form an inclusion compound despite being considerably longer than many molecules that do, presumably because the proximity of the benzene rings would prevent sufficient reduction of strain in the host by positional ordering. At the other end of the scale, the longest guest of the series, didecylbenzene, forms a more conventional disordered inclusion compound at room temperature because the benzene rings are sufficiently well separated to avoid too great a strain on the host. The guests in between these two extremes form superstructures with both longitudinal and orientational ordering of the guests.

REFERENCES

1. L. C. Fetterly, "Non-Stoichiometric Compounds" (L. Mandelcorn, Ed.), Academic Press, New York, 1964.
2. K. D. M. Harris, *J. Solid State Chem.* **106,** 83 (1993).
3. K. D. M. Harris and J. M. Thomas, *J. Chem. Soc., Faraday Trans.* **86,** 2985 (1990).
4. R. Forst, H. Jagodzinski, H. Boysen, and F. Frey, *Acta Crystallogr., Sect. B* **46,** 70 (1990).
5. T. R. Welberry and S. C. Mayo, *J. Appl. Crystallogr.* **29,** 353 (1996).
6. R. Forst, H. Jagodzinski, H. Boysen, and F. Frey, *Acta Crystallogr., Sect. B* **43,** 187 (1987).
7. I. J. Shannon, N. M. Stainton, and K. D. M. Harris, *J. Mater. Chem.* **3,** 1085 (1993).
8. R. Forst, H. Boysen, F. Frey, H. Jagodzinski, and C. Zeyen, *J. Phys. Chem. Solids* **47,** 1089 (1986).
9. R. Lefort, J. Etrillard, B. Toudic, F. Guillaume, T. Breczewski, and P. Bourges, *Phys. Rev. Lett.* **77,** 4027 (1996).
10. M. E. Brown, J. D. Chaney, B. D. Santarsiero, and M. D. Hollingsworth, *Chem. Mater.* **8,** 1588 (1996).
11. M. D. Hollingsworth, M. E. Brown, A. C. Hillier, B. D. Santarsiero, and J. D. Chaney, *Science* **273,** 1355 (1996).
12. Y. Chatani, Y. Taki, and H. Tadokoro, *Acta Crystallogr., Sect. B* **33,** 309 (1977).
13. Y. Chatani, H. Anraku, and Y. Taki, *Mol. Cryst. Liq. Cryst.* **48,** 219 (1978).
14. R. M. Lynden-Bell, *Mol. Phys.* **79,** 313 (1993).
15. M. Rehahn, A.-D. Schlüter, and W. J. Feast, *Synthesis* 386 (1988).
16. Y. Sonoda and K. Kaeriyama, *Bull. Chem. Soc. Jpn.* **65,** 853 (1992).
17. D. D. Perrin and W. L. F. Armarego, "Purification of Laboratory Chemicals," 3rd ed. Pergamon Press, Oxford, 1988.
18. M. Moreno-Manas and A. Trius, *Bull. Chem. Soc. Jpn.* **56,** 2154 (1983).
19. J. C. Osborn and T. R. Welberry, *J. Appl. Crystallogr.* **23,** 476 (1990).
20. R. A. Wood, G. E. Tode, and T. R. Welberry, *J. Appl. Crystallgr.* **18,** 371 (1985).
21. H. L. Casal, *J. Phys. Chem.* **94,** 2232 (1990).
22. K.-J. Lee, W. L. Mattice, and R. G. Snyder, *J. Chem. Phys.* **96,** 9138 (1992).
23. R. L. Vold, R. R. Vold, and N. J. Heaton, *Adv. Magn. Reson.* **13,** 17 (1989).